Butanol-Gasoline Blend and Exhaust Gas Recirculation, Impact on GDI Engine Emissions

Hergueta Santos-Olmo, Cruz; Bogarra Macias, Maria; Tsolakis, Athanasios; Essa, Khamis; Herreros, Jose

DOI:
10.1016/j.fuel.2017.07.022

Butanol-Gasoline Blend and Exhaust Gas Recirculation, Impact on GDI Engine Emissions.

Hergueta C. [1], Bogarra M. [1], Tsolakis A. [1]*, Essa K. [1], Herreros J. M.[1]

[1]Mechanical Engineering, University of Birmingham, B15 2TT, Birmingham, UK;

Email: a.tsolakis@bham.ac.uk

Abstract

A potential approach for addressing simultaneous reductions in toxic pollutants, greenhouse gas emissions and fuel consumption in gasoline direct injection (GDI) engines is the use of renewable alternative fuels. Furthermore, the combination of cleaner fuels with well-established technologies such as Exhaust Gas Recirculation (EGR) can reduce pollutant emissions and improve engine's efficiency.

In this research, the effect of 33% v/v of butanol in EN228 commercial gasoline containing 5% of ethanol (B33) and gasoline (B0) fuels under maximum admissible EGR rate at two steady state engine load (low and medium) conditions has been investigated. B33 reduces engine out carbonaceous emissions, while maintaining similar levels of nitrogen oxide emissions when compared to standard gasoline combustion. However, the physical and chemical properties of butanol (i.e. viscosity and heat of vaporization) showed a negative impact on carbon monoxide emissions at low load due to combustion inefficiencies. The addition of EGR showed a general reduction of gaseous emissions and particulate matter (except unburned hydrocarbons), a trend that was more significant for B33 at medium load. In addition, transmission electron microscope (TEM) analysis showed that B33 is formed by more similar primary particles than primary particles formed with gasoline fuel. From the engine point of view, EGR improved both Brake Specific Fuel Consumption (BSFC) and Brake Thermal Efficiency (BTE) for the studied fuels with respect to baseline conditions.

Keywords: GDI engine, Butanol, EGR, gaseous emissions, particulate matter, TEM

Nomenclature

aTDC	After Top Dead Centre
BSFC	Brake Specific Fuel consumption
bTDC	Before Top Dead Centre
BTE	Brake Thermal Efficiency
CAD	Crank Angle Degree
COV of IMEP	Coefficient of Variation of Indicate Mean Effective Pressure

dp_0	Primary particle diameter
ECU	Engine Control Unit
EGR	Exhaust Gas Recirculation
EVO	Exhaust Valve Opening
GDI	Gasoline Direct Injection
GNMD	Geometric Number Mean Diameter
HC	Hydrocarbons
IVO	Intake Valve Opening
MFB	Mass Fuel Burned
PAH	Polycyclic Aromatics Hydrocarbons
PM	Particulate Matter
TEM	Transmission Electron Microscopy
THC	Total Hydrocarbons
TWC	Three Ways Catalyst

1. Introduction

Gasoline Direct Injection (GDI) engines are fuel efficient and contribute to the reduction of carbon dioxide (CO_2) when compared to port fuel injection engines. The reasons are increased compression ratio by the charge cooling effect of the direct fuel injection, lower pumping losses, higher volumetric efficiency and more accurate injection control [1]. GDI engines also reduce pre-ignition and knock tendency as the compression temperatures are lower, and thus an enhancement in thermal efficiency by a reduction of heat losses can be achieved [2]. On the other hand, GDI engines have reported to increase the concentration of the Particulate Matter (PM) emissions [3, 4]. The main sources of PM formation in GDI engines are identified as fuel piston wetting, injector fuel deposits and inadequate air-fuel mixing. Consequently, the diffusive combustion of rich-in-fuel areas promotes PM formation [5, 6], and also wall wetting by fuel impingement also produces an increment of unburned hydrocarbons (HCs) and carbon monoxide (CO) due to a significant grade of incomplete combustion [7, 8]. For this reason, emission standards such as Euro 6c, which includes a strict limit of $6x10^{11}$ particles per kilometer and comes into force in September 2017 [9], are boosting the development of new technologies to reduce emissions in GDI.

A feasible short-to-midterm solution for addressing additional emissions reduction with a decreased in the demand of high quality fossil fuels is to use renewable bio-alcohols fuels such as

butanol, which is considered a second generation of renewable transportation fuel [10]. Butanol provides complementary physicochemical properties to gasoline blends for decreasing regulated emissions as well as improving combustion. Amongst these properties, higher octane number and oxygen content extend the knock limit for advanced spark timings [11] and improve combustion efficiency, respectively, leading to further CO and total hydrocarbons (THCs) reductions [3, 12]. Furthermore, butanol's higher latent heat of vaporization results in further cooling charge effect in GDI engines, which increases the volumetric and thermal efficiency [13]. The higher latent heat of vaporization combined with its lower adiabatic flame temperature can also assist in NOx reduction [14, 15]. By contrast, studies have reported an increase of NOx with 35% butanol and advanced ST [16, 17], or even insignificant differences in NOx emission [18]. Conversely, butanol's high latent heat of vaporization and viscosity can also have a negative effect on engine operability, associated with engine's cold-start and ignition problems [19]. The lower energy density of bio-alcohols (22% lower butanol than for gasoline) leads to a penalty in fuel consumption and, in most cases, Brake Specific Fuel Consumption (BSFC) increases [20]. Butanol can also be an approach in satisfying the regulated PM levels in modern engines due to its oxygen content, inhibiting particle formation and promoting oxidation rates [21]. In the literature, butanol blends have been reported to reduce large particles (40-60nm), while the formation of small particles (30nm) is promoted [22]. Transmission Electron Microscopy (TEM) has extensively been used for the analysis of the PM size, morphology and nanostructure of soot particles, as these parameters are directly related to the formation process of the particles [23]. However, there are still limited studies on the morphology of butanol-gasoline fuels. This information can provide a guide of the soot oxidation rate, as it depends on the aggregate surface area to volume ratio. It has been estimated that the aggregate surface area to volume ratio, is inversely proportional to primary particle diameter [24]. Therefore, small primary particles will lead to high aggregate surface area favoring soot oxidation [25].

EGR is a widespread technique firstly used in diesel engines to limit thermal NOx formation rate by reducing combustion temperature [26]. However, this technology is primarily implemented in GDI engines to obtain high engine efficiency and to improve fuel economy, since throttling losses can be reduced at low/part load range [27]. EGR increases the overall charge mass so the volumetric

efficiency and the total heat capacity is relatively raised, leading to reduced pumping losses and lower temperature of the in-cylinder walls [28]. EGR has also shown beneficial effects on decreasing the severity of knock in GDI engines [22], enabling to advance the spark timing that improves the combustion phasing and therefore, increasing the engine work output and the thermal efficiency [29]. However, EGR addition slows down the combustion speed, leading to prolonged combustions that occurs over a greater proportion of engine cycle, thereby, worsening combustion stability [30].

In terms of emissions, EGR is reported to improve regulated emissions except for THC, mainly due to the high EGR heat capacity that reduces the HC oxidation rate and may cause engine to misfire when high EGR rates are used [29, 31]. The effect of EGR on particle emissions in GDI engines has been also reported. Depending on the engine condition and EGR ratio, some authors have reported that EGR addition increases the accumulation mode of particles and reduce nucleation mode (medium loads) [32]. This effect was attributed to the lower in-cylinder temperature that reduced the soot oxidation rate. This effect appeared to be more significant than the decreased in primary carbon particles formed by thermal pyrolysis and dehydrogenation reaction of fuel vapor droplets, and thus, the accumulation mode is increased. However, other authors have found the opposite effect, with reduced accumulation mode and increased nucleation mode when EGR ratio was higher than 12% [22, 32]. It was attributed to the low in-cylinder temperature that limited the primary particle formation by thermal pyrolysis and dehydrogenation. Additionally, the abruptly increased in HC, which are highly related to nucleation mode, promoted further the increment of small particles and consequently, the reduction in accumulation mode relatively to nucleation mode. Others have found reduction of 46% and 90% in particle number (PN) and solid particle number, respectively, at high load and slightly rich condition that simulate the transient engine conditions with cooled EGR [33].

Although, the use of alcohols for replacing gasoline in the GDI engines has been studied, there is still a need to better understand the behavior and the potential benefits of butanol fuel in these engines in terms of emissions reduction and combustion performance. The aim of this investigation is to assess and to further the understanding on the effect of the utilization of high butanol fraction blends on combustion characteristics, gaseous and particulate matter emissions in GDI engines. The potential benefits of high-diluted combustion process with EGR are also investigated in conjunction

with the B33 fuel. Additionally, the analysis of the primary particle diameters of the PM agglomerates emitted for both fuels has also been investigated through transmission electron microscopy (TEM).

2. Materials and Methods

An 2L air-guided, four cylinders turbocharged GDI engine manufacturer by Ford has been used for this study. The engine was coupled to a 75kW AC dynamometer and inverter drive capable of motoring and absorption/regeneration. The specifications are depicted in Table 1 and the schematic of the engine and experimental set up is shown in Figure 1.

Table 1: GDI engine specifications

Engine Specifications	
Compression Ratio	10:1
Bore×Stroke	87.5× 83.1 mm
Turbocharger	Borg Warner k03
Rated Power	149kW at 6000rpm
Rated Torque	300Nm at 1750-4500rpm
Engine Management	Bosch ME 17

The engine was operated at stoichiometric conditions where the oxygen concentration was controlled by a Heated Exhaust Gas Oxygen (HEGO) sensor. An AVL miniature piezo-electric pressure transducer referenced to the engine cycle utilizing a Baumer 720 pulse per revolution magnetic encoder was used for in-cylinder pressure measurements, considering an average of 200 cycles. The in-cylinder pressures were acquired using an in-house LabView application. Fuel consumption was monitored with a Rheonik RM015 Coriolis fuel meter. The fuel supply temperature control was provided by a fuel conditioning unit sourced from CP Engineering, and set to 28°C for the test. The OEM's calibration strategy to reduce pumping losses was the utilization of valve overlapping to increase the residuals. This technique is known as internal EGR, where the intake valve opening (IVO) was set at 11 CAD bTDC (Crank Angle Degree before Top Dead Centre), and the exhaust valve closing (EVO) is at 57 CAD aTDC (Crank Angle Degree after Top Dead Centre). The engine is also equipped with high pressure external EGR system (designed and implemented by the University of Birmingham). The external EGR valves were controlled using a standalone control

unit that requires a pulse-width modulated input signal to specify the desired valve position, provided by a custom LabView application.

A Fourier Transform Infrared Spectroscopy (FTIR) 2100 MKS was used to measure gaseous emissions (CO, CO_2, NOx and THC). The sample was previously filtered to avoid potential damage of the optical lenses by PM, and pumped via a heated line maintained at 190°C to prevent any water and HC condensation. The EGR ratio was determined using eq.1 by utilising an AVL Digas 440 non-dispersive infrared analyzer, to measure the CO_2 concentration at the intake and exhaust.

$$EGR\ Ratio = \frac{CO_{2(intake)}}{CO_{2(exhaust)}} \cdot 100\ (\%) \quad (1)$$

Particle size distribution measurements were carried out using a TSI scanning mobility particle size composed by a series 3080 electrostatic classifiers, a 3081 Differential Mobility Analyzer and a 3775 Condensation Particle Counter. The sample flow and the sheath flow were set to 1 and 10 lpm respectively. The distribution ranged from 7.5 to 294 nm. The sampling point was located pre-three way catalyst (TWC). To prevent HCs and water condensation, the line temperature was also maintained at 190 ℃ during the test. The samples were then diluted with air at a dilution ratio of 7-8, using an ejector diluter system, fitted with a high efficiency particulate arrestance filter to precondition the sample.

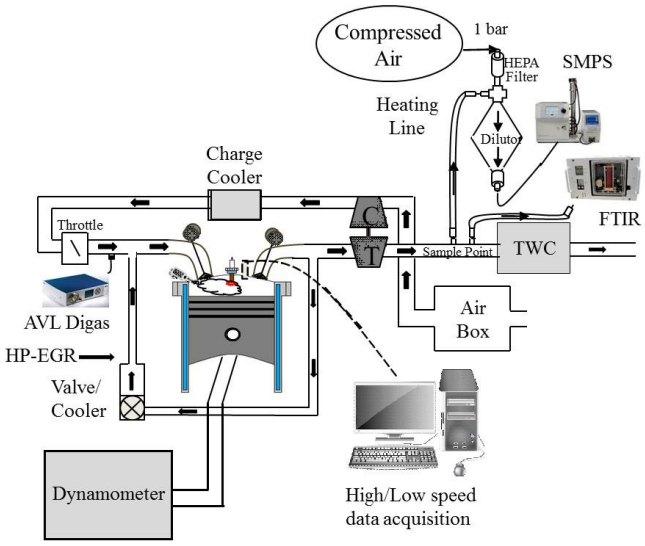

Figure 1: Schematic of the engine and instrumentation set up

A custom post-processing script was developed in Matlab to import and time-align the channels of data obtained by the multiple data acquisition sources. The Matlab function enabled a detailed combustion process analysis by means of in-cylinder pressure measurements, including heat release rate, mass fraction burned (MFB), in-cylinder pressure, total cycle indicated mean effective pressure (IMEP) and coefficient of variation (COV) of IMEP (%).

For the PM primary particles analysis 3.05mm TAAB Formvar coated cooper grids were used to obtain the sample. The grids were directly exposed in the engine exhaust pipe before the three-way catalyst. A JEOL 1200EX TEM LaB6 80keV operating voltage was used to obtain the micrographs for primary particle analysis.

3. Experimental Procedure

The engine was operated at two steady-state conditions from the New European Driving Cycle for a mid-size/large family vehicle with 2L engine under urban driving operation: a) 35Nm/2100rpm (low load) and b) 60Nm/2100rpm (medium load). Butanol-gasoline fuel was blended at the University of Birmingham using standard EN228 gasoline with 5% (v/v) ethanol content (B0) and pure n-butanol was used in the process. The fuel characteristics are listed in Table 2.

Table 2: Fuels properties [34-36]

Property	**Gasoline**	**n-Butanol**
Chemical formula	$C_{5.88}H_{11.06}O_{0.1}$ [a]	$C_4H_{10}O$
Density (kg/m^3)	743.9 [a]	811
Research octane number	96.8 [a]	96
Motor octane number	85.2 [a]	85
Latent heat of vaporization (kJ/kg)	350	722
Lower Heating Value LHV (kJ/kg)	42.2 [a]	33.1
Auto-ignition temperature (℃)	~300	385
Laminar flame speed (m/s)	51	58.5
Viscosity (mm^2/s) at 40℃	0.4-0.8	2.63
Adiabatic flame temperature (K)	2370	2340

[a] Provided by Shell

The blend chosen was 33% v/v (B33) of butanol in EN228 commercial gasoline containing 5% of ethanol. An IKA C200 calorimeter was used to measure the lower heating value of B33. The result

obtained was 40.175 MJ/kg. The test was repeated three times to ensure reproducibility and repeatability, with a maximum relative standard deviation of 0.1% between the measurements.

The spark timing was varied to phase the MFB50% to the one obtained for baseline gasoline for Maximum Brake Torque (8± 1.5 CAD aTDC timing) for comparison purposes (Table 3). Camshaft timings were fixed at short overlap setting to avoid the presence of residuals in the combustion chamber (IVO 11 CAD bTDC and EVC 8 CAD aTDC). The effect of butanol on gasoline was studied under the influence of external EGR. The conditions must satisfy the constrain of remaining COV of IMEP below 3% at maximum EGR, which is a reasonable measurement of a modern engine stable operation [35]. Prior to the test, the engine was warmed up, starting the measurement at 95±0.5 °C for coolant and 95±2 °C for oil. The intake air temperature was maintained at 45±1 °C throughout the experiment to reduce the test-to-test variability. Otherwise, the standard Engine Control Unit (ECU) calibration settings were used such as injection timing. Confidence intervals using a 95% confidence level, which reflects the reliability and repeatability, have been calculated for gaseous emissions. All experiments were conducted on the same day for each condition to reduce the effect of day-to-day variability of the engine and emissions equipment on the results obtained.

Table 3: Engine conditions and ECU settings

			Ignition Timing CAD bTDC	**EGR (%)**	**Spark Timing CAD bTDC**	**MFB50% CAD aTDC**
35Nm/2100rpm	B0	Baseline	304.5	0	30.75	9.4
		Max %EGR	304.5	17	+49.5a	9.12
	B33	Baseline	304.5	0	33	9.14
		Max %EGR	304.5	17	+50.25a	8.38
60Nm/2100rpm	B0	Baseline	303.7	0	30	7.7
		Max %EGR	303.7	19	+49.5a	7.04
	B33	Baseline	303.7	0	29.7	6.9
		Max %EGR	303.7	19	+50.75a	7.9

+ advance with respect to ECU settings

The study of the primary particle diameters (dp_0) for B33 and gasoline fuels where carried out at 60Nm/2100rpm. For the analysis of dp_0, manual measurements were performed, although it was only measured the apparently identifiable primary particles were measured. The recognition of the primary particles boundaries is somewhat subjective, and can lead to some fluctuations in the analysis of the results [37]. Additionally, the sample has to be large enough to ensure its log-normality distribution,

as Gaddam et al. [38] have discussed. At least 240 primary particles were considered per fuel, located in 17 different agglomerates randomly chosen in the TEM grids. One-sample non-parametric Kolmogorov Smirnov test in the IBM statistical package for social sciences software (SPSS) was performance to check the log-normality.

4. Results

4.1 Combustion studies

The in-cylinder pressure and heat release rate for B33 are overlapped with respect to those obtained under gasoline fueling at 35Nm (Figure 2 (a)). In addition, the MFB50% timing was kept identical (Figure 3 (a)) by slightly advancing the spark timing (Table 3), so comparisons of the two fuels engine-out emissions can be made based on their chemistry. It has been previously reported that the higher flame speed of butanol promotes stable combustion and improves the degree of constant volume heat release [34]. However, at this engine load, it seems that the fuel physical properties (i.e. viscosity and enthalpy of vaporization) dominate over the faster laminar burning velocity of butanol (Table 2) resulting in advanced spark timing (2.25^{o} CAD) to achieve the same MFB50% (Figure 3 (a)) and slightly worse combustion stability as COV of IMEP indicates (Figure 4). It is thought that the high viscosity of B33 impacts on the fuel spray atomization process, promoting more in-homogeneous mixture and hence, it reduces combustion stability.

For the medium engine load of 60 Nm, the in-cylinder peak pressure and heat release rate of B33 were slightly higher compared to gasoline, which is in agreement with the results reported earlier in literature [12, 22, 36, 39], at a comparable combustion phasing (Figure 3 (a)). The higher fuel spray velocities, resulting from the increased engine load at 60 Nm, created a turbulent motion inside the cylinder that promoted the homogeneity of the air-fuel mixture [39]. At this engine load, the higher laminar burning velocity of butanol combined with an enhancement in fuel spray atomization provide greater combustion quality when compared to gasoline, as observed by the lower COV of IMEP (Figure 4).

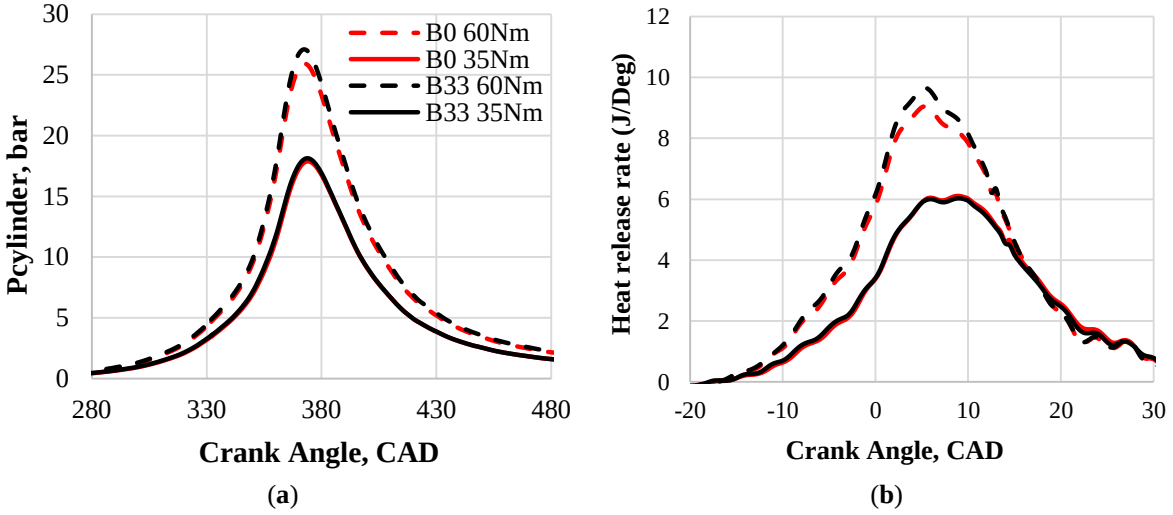

203 **Figure 2:** (a) In-cylinder pressure and (b) heat release rate versus CAD for gasoline (B0) and B33 at 2100rpm

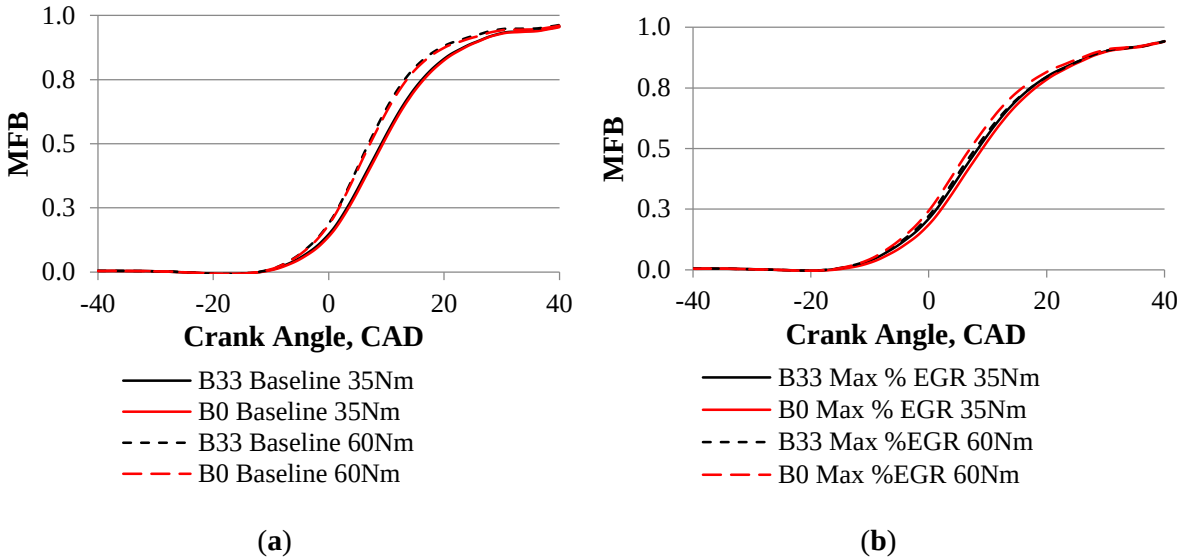

204 **Figure 3:** MFB for Gasoline and B33: (a) Baseline and (b) Max EGR at 2100rpm

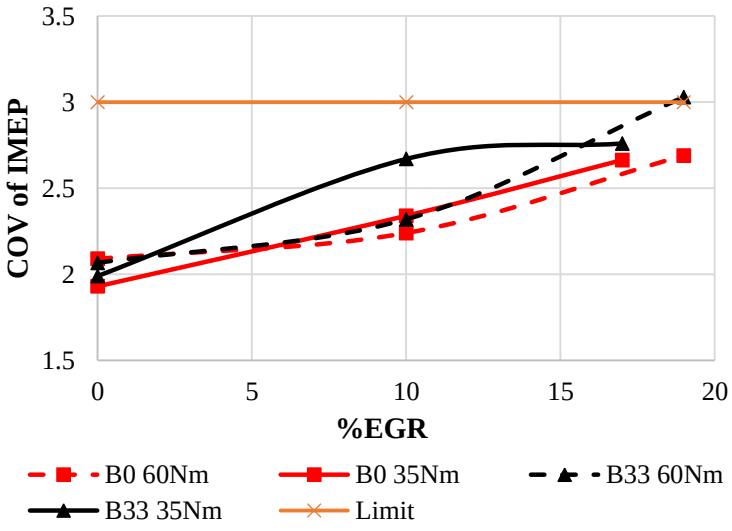

205

Figure 4: COV of IMEP as a function of EGR rate (%) at 2100rpm

The introduction of maximum applicable EGR rate (%) in B33 fueling at low and medium engine load slightly reduced the in-cylinder pressure and heat release with respect to maximum EGR with gasoline fuel (Figure 5). The B33 higher cooling charge capability together with the EGR negatively affected the fuel vaporisation of B33, and consequently the mixture homogeneity as reflected in the COV of IMEP (Figure 4), which leads to marginal peak reduction in both, the in-cylinder pressure and heat release rates.

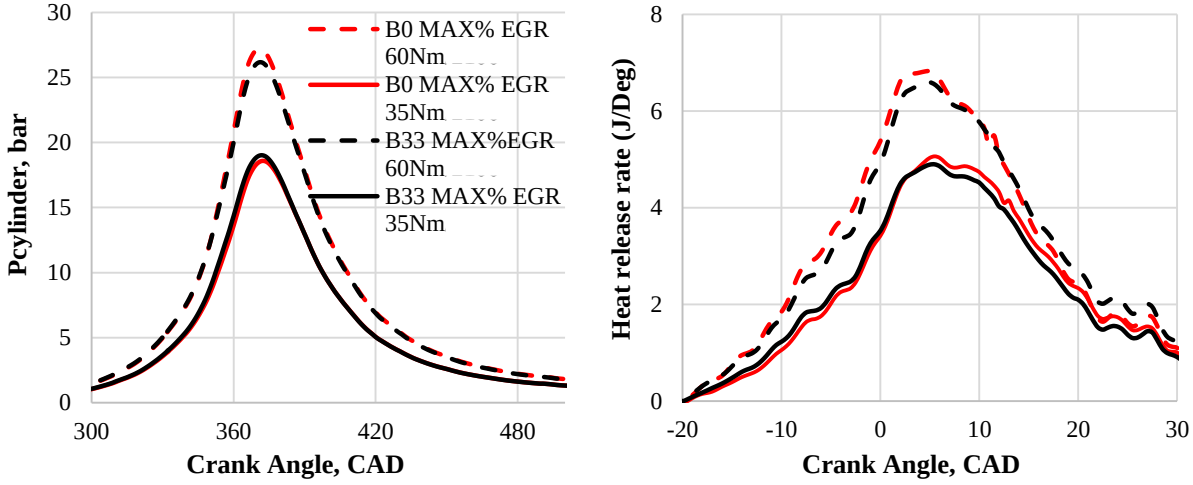

Figure 5: (a) In-cylinder pressure and b) heat release rate versus CAD for Gasoline and B33 at maximum EGR and 2100rpm

Figure 6 (a) shows that the EGR enhances the BSFC for both fuels, in agreement with the literature [8, 32]. When EGR is used, the throttle valve must be further opened in order to maintain the oxygen level at stoichiometric ratio and therefore, the pumping losses are reduced. In all cases, the BSFC of B33 combustion was higher in comparison to gasoline combustion. The brake thermal efficiency, which is inversely proportional to the BSFC, and considers the lower heating value of the fuel blends is shown in Figure 6 (b). There are no significant differences in the indicated thermal efficiency which concludes that the higher BSFC in the case of the B33 blend is due to the lower energy density of butanol compare to gasoline [36].

As it can be observed from the reduction of the exhaust gas temperatures (Figure 7), EGR brings the in-cylinder temperature down, enabling a reduction of the heat losses to the coolant and

surroundings, and contributing in further improvements of the brake thermal efficiency (BTE) [22, 32]. Thus, EGR enhances BTE (Figure 6 (b)) for the gasoline and B33 combustion at both engine loads. Although B33 worsens the BSFC compared to gasoline, the higher heat of vaporization of B33 can improve the volumetric efficiency and reduce the heat losses to the coolant and surroundings. The physicochemical properties of butanol in gasoline blend is reflected in a BTE similar than for gasoline as the differences are around 1% at both engine conditions (Figure 6 (b)).

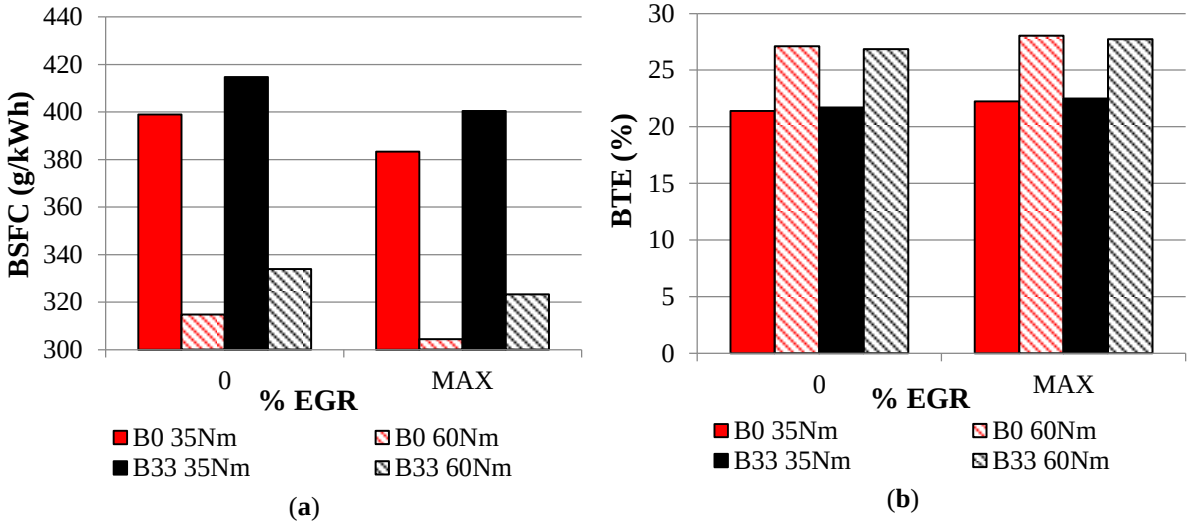

Figure 6: a) Brake Specific Fuel Consumption BSFC and b) BTE with and without max %EGR ratio at 2100rpm.

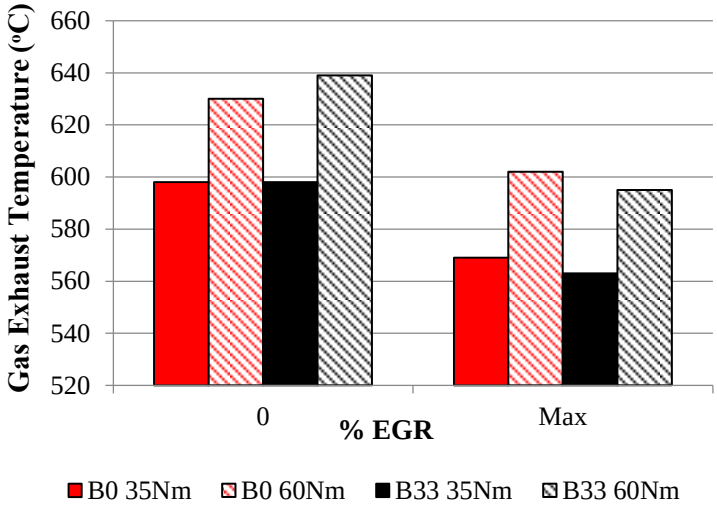

Figure 7: Exhaust gas temperature at baseline and max % EGR at 2100 rpm

4.2 Gaseous Emissions

THCs and CO emissions provide a direct insight into the combustion process by contributing to the evaluation of the combustion efficiency. The combustion of B33 at 35Nm resulted in slightly lower THC emissions compared to gasoline (Figure 8). Although both the oxygen content of B33 and its shorter carbon chain length are promoting higher oxidation rates to CO_2, the poor butanol spray and mixing properties at low load inhibit this oxygen effect, increasing CO emissions [40] through incomplete combustion. A significant decrease in THC and CO is noticeable at 60Nm (Figure 9) with the combustion of B33 compared to gasoline. The greater combustion stability, as it can be observed from the COV of IMEP and, higher combustion temperature and heat release rate may be the reasons. The exhaust gas temperature of B33 at 60Nm raised by nearly 10 °C (Figure 7) with respect to gasoline combustion, which is an indication of higher in-cylinder temperature for B33. This resulted in a THC and CO reduction of 12.6% and 4%, respectively, as greater oxidation rates of the THC can be achieved during the combustion and exhaust stages.

The in-cylinder pressure increases with EGR, and as a result, the fuel is forced into the piston ring crevices that then is released as unburnt HC emissions during the exhaust stroke [7]. Furthermore, the reduction of combustion temperatures induced by the addition of EGR led to lower heat release and combustion stability. This promotes lower oxidation of THC during the combustion process and exhaust stroke. In addition, the lower mixing time available for fuel-air mixture due to spark timing advance (a total average of 50 CAD advanced, see Table 3) can also result in poorer mixture preparation, which worsens the oxidation of THC [32] for both fuels. The combustion of gasoline at maximum EGR produced higher THC concentration for both engine conditions, even when the stability and exhaust temperature was less favourable for B33. This effect has been reported in literature for EGR rates up to 20%, THCs were found to decrease with the increasing bio-alcohol content [22]. CO emissions were generally reduced with EGR addition compared to baseline combustion for both fuels and engine conditions. A reason could be the reduction of liquid fuel [41] due to a drop in pumping losses. Furthermore, THC oxidation is highly worsened respect to baseline (Figure 8), which leads to lower CO and CO_2 emissions. CO emissions for B33 experienced a

significant reduction in both conditions at maximum EGR rate, accounting for 6.73% and 14.76% at 35Nm and 60Nm respectively, compared to gasoline.

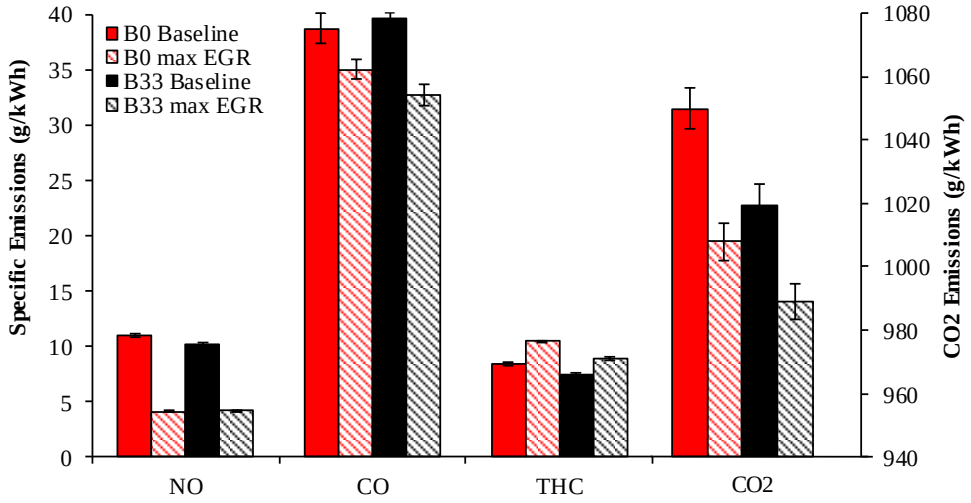

Figure 8: Specific gaseous emission for baseline and maximum EGR ratio at 35Nm/2100rpm for B33 and B0

NOx emissions keep a clear trend at 35 Nm where a decrease of 7.65% in NOx was observed for B33; however, no significant reduction was seen at 60 Nm. At low load, the exhaust gas temperature of both fuels (Figure 7) were the same, which can indicate a narrow difference of in-cylinder temperature (source of thermal NOx formation). However, the exhaust gas temperature is not a direct measurement of the in-cylinder temperature, and no accurate prediction can be made based on an insignificant difference in exhaust gas temperature. Thus, it is thought that butanol's lower adiabatic flame temperature of B33 could reduce the local combustion temperatures compared to gasoline, being the reason for slightly NOx reduction [36, 42] at 35Nm. In addition, the marginally lower heat release rate at the end of the combustion phase could potentially reduce the NOx emissions with respect to gasoline. On the other hand, the reason for the lack of effect of B33 at 60 Nm could be the better homogenisation and stability, enabling to gain higher combustion temperature and heat release rate (Figure 2) as it can be predicted through the exhaust temperatures (Figure 7) in this case [14].

EGR reduces NOx emissions for both fuels. The general reason is the higher overall heat capacity in the combustion chamber limits the combustion temperature, and consequently the thermal NOx formation rate. Comparing both engine conditions and fuels at maximum EGR, there was a clear

reduction in NOx of 37% at 60Nm by B33 (Figure 9), while there was not benefit in reduction of NOx at low load (Figure 8). Assuming that the in-cylinder temperature with EGR is lower in both engine conditions for B33, which is reflected in exhaust gas temperature (Figure 7), it could be thought that NOx emission for B33 must be lower than in the gasoline case. However, this is not observed in both engine conditions. The high viscosity of butanol together with the low injection pressure at 35Nm worsens the spray pattern and hence, the air-fuel mixture quality. Consequently, the combustion of B33 is more unstable compared to gasoline at low load. This has been reported to promote diffusive flames (precursor of NOx emissions), and as a result, inhibiting the favourable influence of the cooling charge effect of B33 for NOx inhibition [28].

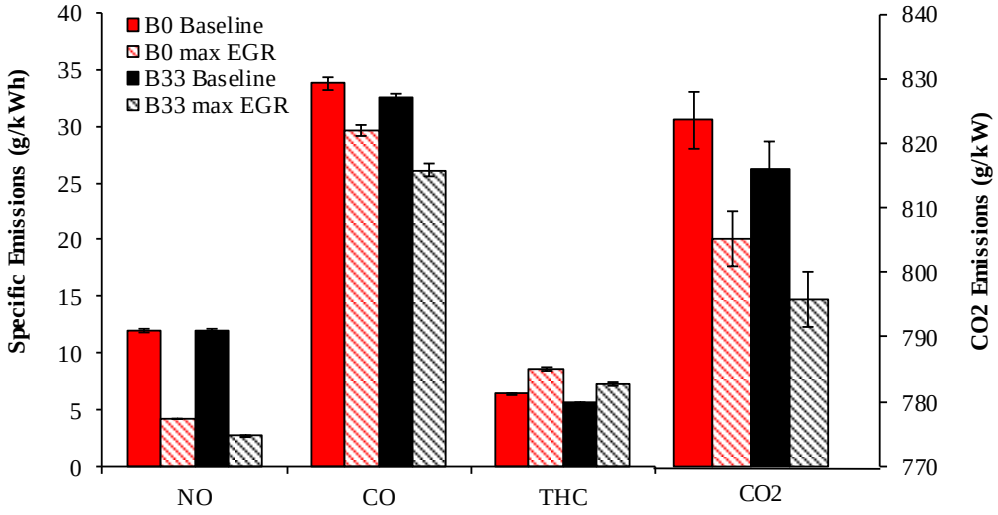

Figure 9: Specific gaseous emissions for baseline and maximum EGR at 60Nm/2100rpm for B33 and B0

The combustion of B33 provided a reduction in CO_2 emissions at both loads when compared to gasoline. The decrease in CO_2 emissions with the butanol blend is due to the higher H/C and O/C ratio of B33 with respect to gasoline fuel. The CO_2 reduction is more noticeable at low load which could be attributed to a lower conversion of THC to CO_2 due to the lower combustion efficiency and lower carbon fuel content. With EGR, CO_2 experienced a reduction for both fuels. The EGR improved BSFC (Figure 6 (a)) and, consequently; a lower mass of fuel is needed to maintain the engine operation condition. In addition, the incomplete combustion of THCs, which increases its emissions, may be another cause of CO_2 reduction. At both conditions with EGR, B33 produced lower CO_2

emissions, which can be again ascribed to its higher H/C and O/C ratios and improved volumetric efficiency due to the greater cooling charge effect with respect to baseline operation.

4.3 PM Emissions

Particle number size distribution from the combustion of B33 and gasoline with and without the addition of EGR at maximum rates are plotted in Figure 10. At low engine load (Figure 10 (a)) during baseline combustion, a unimodal particle distribution. Firstly, B33 provided a significant reduction in particle concentration compared to gasoline, accounting for 60% when the peak was considered at 35Nm. At this engine condition, gasoline particle size distribution is displaced to larger diameters with respect to B33 results. The combustion of B33 presents a peak governed by nucleation mode particles with the geometric number mean diameter (GNMD) being at 30nm, exhibiting a reduction in size, mass and number of particles relative to gasoline. The accumulation mode of particles has a close relation to the polycyclic aromatic hydrocarbons (PAHs) as it has been reported in literature [1, 3, 43, 44]. Thus, the addition of butanol to the gasoline, reduces the aromatics content in the fuel blend, and consequently, the number of particles with high GNMD is decreased, favoring the increased number of nuclei particles [39]. In addition, the presence of oxygen as part of the alcohol fuel reduces the soot formation rate and enlarges the oxidation rate during the combustion process. Hence, the reductions of number and GNMD for B33 combustion decrease the number of interaction between the particles, leading to lower surface growth, coagulation and aggregation processes, and therefore the presence of large hydrocarbons for the formation of the accumulation mode particles decreases.

Similar results were found at 60 Nm (Figure 10 (b)), but in this case the reduction in the peak of the particle distribution was even more notable, accounting for 81% with respect to gasoline. This engine condition promoted a more homogeneous air-fuel mixture for B33, which resulted in higher combustion efficiency and stability (Figure 4). This enhancement in the stability was reflected in higher in-cylinder pressure and heat release that indicate higher combustion temperatures shown by exhaust gas temperatures in (Figure 7). Therefore, the soot and THC oxidation rate is increased, enabling a greater difference between gasoline and B33 at 60Nmwith respect to 35Nm.

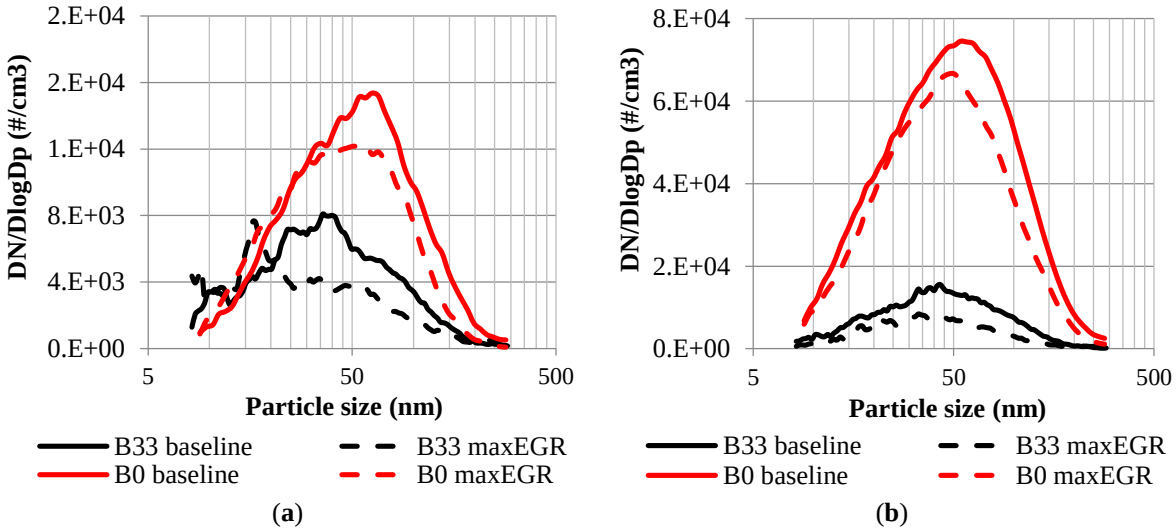

Figure 10: Effect of B33 and maximum EGR ratio on particle size distribution: a) 35Nm/2100rpm and b) 60Nm/2100rpm

A general reduction of particle number and size was achieved under EGR conditions. A reasonable explanation for lower PM formation can be attributed to the fact that EGR generally improves engine efficiency and fuel consumption (Figure 6). Therefore, for a given engine load, less fuel is required into the cylinder compared to baseline condition, leading to proportionally less PM being formed [31]. For both fuels and conditions tested, the particle distribution peak shifts towards smaller particles sizes with the introduction of EGR, indicating a growth in proportion of finer particles in benefit of the reduction in particulate mass. The application of EGR led to a 15-20% reduction in the particle concentration peak of the distribution for both fuels and engine operating conditions. Furthermore, the temperature was reduced by EGR, and consequently primary carbon particles formed by thermal pyrolysis and dehydrogenation reaction of fuel vapor may have been decreased [45]. The consequence is that overall concentration decreased with EGR for both fuels.

4.4 Primary Particle Diameter (d_{p0}) Analysis

As reported in the previous sections, the butanol blends reduce considerably the concentration of PM independently of the engine condition and the size of the final agglomerate. Gasoline PM presents aciniform-shape formed by several nearly spherical primary particles. In this section, an analysis of the effect of butanol in the primary particle diameter (d_{p0}) has been performed at 60Nm/2100rpm, in which the PM concentration was more significantly reduced. An example of the TEM micrograph of

particles collected from the GDI engine exhaust for both fuels is shown in Figure 11. Previous studies reported the presence of different types of particles in GDI engines: i) nearly-spherical HCs droplets, ii) solid spherules as small as 6 nm, iii) 'wet' diesel-like particles and iv) 'dry' diesel like particles [46, 47]. These types of particles were also found in B33 in this research work.

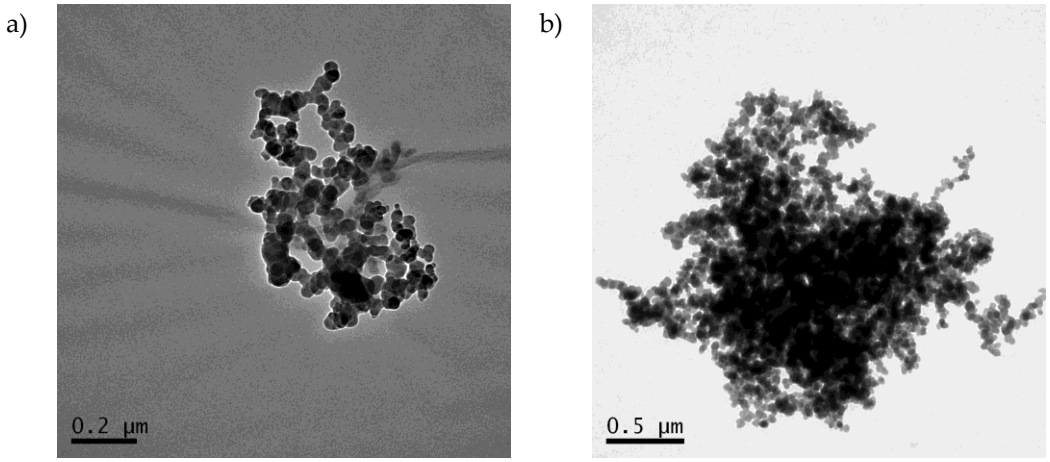

Figure 11: TEM micrographs of PM at 60Nm/2100 engine condition at standar calibration for: a) B33 and b) Gasoline

The log-normal primary particle size distribution for B33 and gasoline obtained by IBM statistical package for social sciences (SPSS) software are shown in Figure 12. B33 particle agglomerates are formed by similar mean diameter primary particles as the normal log shows. At this engine condition, B33 combustion led to higher in-cylinder pressure (Figure 2, and thus, likely higher in-cylinder temperature (as the exhaust temperature trends also indicates) that could increase the rate of particle formation (although also the rate of oxidation), favoring the formation of primary particles with higher diameters [23]. However, the presence of oxygen in B33 seems to counteract this effect, maintaining the size of the formed primary particles the same as the ones recorded from the gasoline combustion. The oxygen content in bio-alcohols fuels can reduce the soot formation rate and enhance the formed particles oxidation rates during the combustion process, [21]. These results are similar than the found for diesel bio-alcohol fuels combustion as reported in literature [48, 49], where in these cases, bio-alcohols even showed slightly lower primary particles diameters due to the oxygen content. Therefore, the oxygen content in B33 is likely to be helpful to limit the rate of primary particles formation.

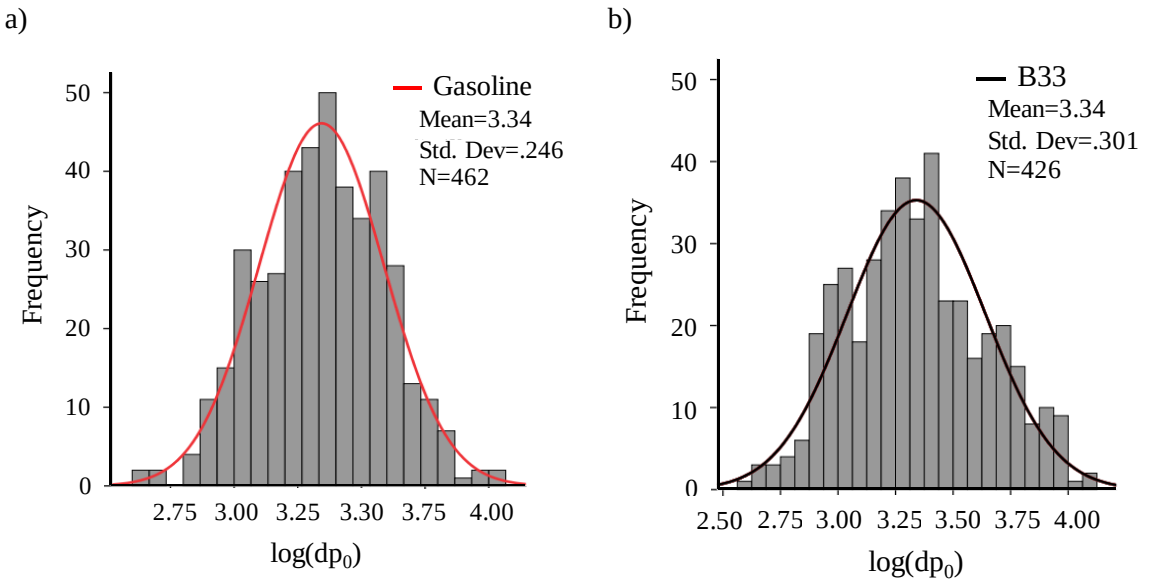

Figure 12: Primary particles size distributions at 60Nm/2100rpm for: a) Gasoline and b) B33

Additionally, the mean primary diameter and standard deviation achieved from the primary particles size distribution for B33 and gasoline are plotted in Figure 13. The average diameter for B33 was in 28.96 nm while gasoline showed a diameter 29.1 nm, which was also found in our previous work for gasoline [23] . B33 formed a slightly smaller primary particle but the standard deviations overlap. Therefore, it can be concluded that the differences in primary particle diameter are negligible in this study.

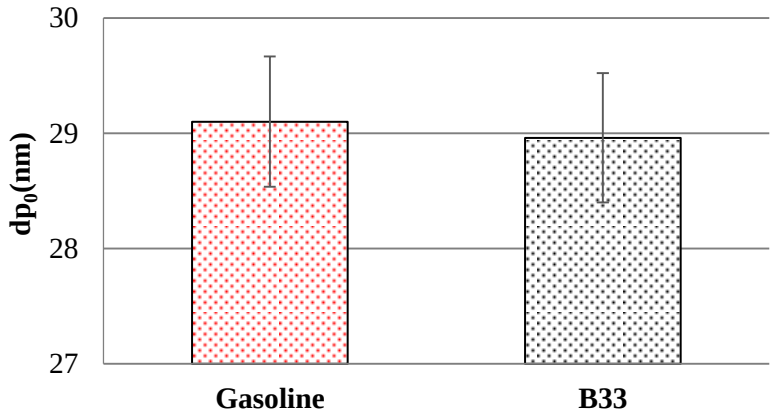

Figure 13: Average primary particle diameter

4.4 Summary of Results

The effect of B33 with and without EGR are shown in Table 4, to present qualitatively the benefits of B33 in comparison to gasoline baseline combustion.

Table 4: Performance combustion of B33 combined with EGR with respect to gasoline combustion: blue + positive, red - negative and - - - insignificant effect.

		BSFC	BTE	COV of IMEP	CO	THC	NOx	CO_2	PM	
B33 35Nm/2100rpm	Baseline	- -	- - -	-	-	+	- - -	++	++	
	17% EGR	-	- - -	- - -	+	- - -	++	++	+	dp_0
B33 60Nm/2100rpm	Baseline	-	- - -	+	+++	+	- - -	++	+++	- - -
	19% EGR	-	- - -	- -	+	- - -	++	++	++	

5. Conclusions

The effect of butanol 33% v/v in EN 228 commercial gasoline containing ethanol 5% v/v (B33) and EGR rate on combustion characteristics and regulated emissions in a multi-cylinder GDI production engine has been investigated. The influence of the butanol addition on the engine combustion characteristics and emissions was dependent on engine operating (i.e. load) conditions. At low engine loads, butanol's physical properties (e.g. high viscosity) are more influential on the combustion performance than its chemical properties (e.g. higher flame speed). Consequently, the combustion of B33 was observed to be more unstable due to the deteriorated fuel spray atomization and in-homogeneous air-fuel mixture, also contributing to the marginally increased carbon monoxide emissions. Conversely, butanol's shorter carbon chain and its oxygen content help to reduce the rest of the emissions. As the engine load was increased, and hence the fuel injection pressure, the combustion performance of B33 was improved through greater air-fuel mixture quality and potentially improved spray atomization; that was reflected in an overall reduction of gaseous and particulates matter emissions.

Transmission Electron Microscope (TEM) analysis showed that B33 did not increase the primary particle diameters, even when the in-cylinder temperature was higher. This confirmed that the oxygen content of butanol could limit the rate of soot formation and at the same time promote soot oxidation. Therefore, in terms of the obtained soot agglomerate surface area to volume ratio, gasoline

and its blends with butanol are expected to have the same impact on the soot oxidation process during the regeneration stages of the Gasoline Particulate Filters. It was shown that B33 was an effective fuel to reduce most of the legislated emissions in both engine conditions, while maintaining engine brake thermal efficiency (BTE).

The addition of EGR provided a general improvement of BTE and brake specific fuel consumption (BSFC) for both fuels and was beneficial to B33 since greater engine-out emissions reduction was achieved.

The research work presented here has shown that high percentages of butanol in gasoline blends combined with EGR technology can be a potential solution in GDI engines for reducing legislated emissions while maintaining the BTE compare to gasoline. However, it is anticipated that the calibration and injection systems of the engine would have to be adapted to minimize its limited performance at low loads, since the physical properties can predominate over its advantageous chemical properties.

Acknowledgments: C.H.S.O. would like to thank University of Birmingham for his scholarship. M.B.M. would like to thank EPSRC (Grant No: 1377213) for providing her scholarship. Innovate UK (Technology Strategy Board) is acknowledged for supporting this work with the project "CO_2 Reduction through Emissions Optimisation" (CREO: ref. 400176/149). The Advantage West Midlands and the European Regional Development Fund as part of the Science City Research Alliance Energy Efficiency Project are also acknowledged for supporting the research work.

References

1. F. Zhao, M.C. Lai, and D.L. Harrington, Automotive spark-ignited direct-injection gasoline engines. *Prog. Energ. Combust.*, 1999. **25**(5): p. 437-562.
2. A.C. Alkidas, Combustion advancements in gasoline engines. *Energ. Convers. Manage.*, 2007. **48**(11): p. 2751-2761.
3. G. Karavalakis, et al., The impact of ethanol and iso-butanol blends on gaseous and particulate emissions from two passenger cars equipped with spray-guided and wall-guided direct injection SI (spark ignition) engines. *Energy*, 2015. **82**: p. 168-179.
4. D.C. Quiros, et al., Particle effective density and mass during steady-state operation of GDI, PFI, and diesel passenger cars. *J. Aerosol Sci.*, 2015. **83**: p. 39-54.

5. C. Wang, et al., Impact of fuel and injection system on particle emissions from a GDI engine. *Appl. Energ*, 2014. **132**: p. 178-191.
6. J.E. Ketterer and W.K. Cheng, On the Nature of Particulate Emissions from DISI Engines at Cold-Fast-Idle. *SAE J-Automot.Eng.*, 2014. **7**(2): p. 986-994.
7. A.O. Hasan, et al., Control of harmful hydrocarbon species in the exhaust of modern advanced GDI engines. *Atmos.Environ*, 2016. **129**: p. 210-217.
8. D.A. Fennell, Exhaus Gas Fuel Reforming for Improved Gasoline Direct Injection Engine Efficiency and Emissions Mechanical Engineering at University of Birmingham, Birmingham, 2014.
9. F. Steimle, et al. "Systematic Analysis and Particle Emission Reduction of Homogeneous Direct Injection SI Engines", 2013-01-0248, 2013.
10. S. Heyne and S. Harvey, Assessment of the energy and economic performance of second generation biofuel production processes using energy market scenarios. *Appl.Energ*, 2013. **101**: p. 203-212.
11. B. Deng, et al., The heat release analysis of bio-butanol/gasoline blends on a high speed SI (spark ignition) engine. *Energy*, 2013. **60**: p. 230-241.
12. Z. Chen, et al., Impact of higher n-butanol addition on combustion and performance of GDI engine in stoichiometric combustion. *Energ.Convers.Manage*, 2015. **106**: p. 385-392.
13. J.M. Bergthorson and M.J. Thomson, A review of the combustion and emissions properties of advanced transportation biofuels and their impact on existing and future engines. *Renew.Sust.Energ.Rev.*, 2015. **42**: p. 1393-1417.
14. R. Feng, et al., Experimental study on SI engine fuelled with butanol–gasoline blend and H2O addition. *Energ.Convers.Manage*, 2013. **74**: p. 192-200.
15. B.R. Wigg, A Study on the Emissions of Butanol Using a Spark Ignition Engine and their Reduction Using Electrostatically Assisted Injection. Mechanical Engineering at University of Illinois, Urbana-Campaign, 2011.
16. B. Deng, et al., The challenges and strategies of butanol application in conventional engines: The sensitivity study of ignition and valve timing. *Appl.Energ*, 2013. **108**: p. 248-260.
17. M. Pechout, M. Mazac, and M. Vojtisek-Lom. "Effect of Higher Content N-Butanol Blends on Combustion, Exhaust Emissions and Catalyst Performance of an Unmodified SI Vehicle Engine", SAE, 2012-01-1594, 2012.
18. T. Wallner, S.A. Miers, and S. McConnell, A Comparison of Ethanol and Butanol as Oxygenates Using a Direct-Injection, Spark-Ignition Engine. *J.Eng.Gas.Turb.Power*, 2009. **131**(3): p. 032802-032802.
19. G. Broustail, et al., Comparison of regulated and non-regulated pollutants with iso-octane/butanol and iso-octane/ethanol blends in a port-fuel injection Spark-Ignition engine. *Fuel*, 2012. **94**: p. 251-261.
20. F. Catapano, et al. "Effects of Ethanol and Gasoline Blending and Dual Fueling on Engine Performance and Emissions", SAE, 2015-24-2490, 2015.
21. E.J. Barrientos, et al., Particulate matter indices using fuel smoke point for vehicle emissions with gasoline, ethanol blends, and butanol blends. *Combust.Flame*, 2016. **167**: p. 308-319.
22. Z. Zhang, et al., Combustion and particle number emissions of a direct injection spark ignition engine operating on ethanol/gasoline and n-butanol/gasoline blends with exhaust gas recirculation. *Fuel*, 2014. **130**: p. 177-188.

23. M. Bogarra, et al., Impact of exhaust gas fuel reforming and exhaust gas recirculation on particulate matter morphology in Gasoline Direct Injection Engine. *J. Aerosol Sci.*, 2017. **103**: p. 1-14.
24. T.L. Barone, et al., Inertial deposition of nanoparticle chain aggregates: Theory and comparison with impactor data for ultrafine atmospheric aerosols. *J. Nanopart. Res.*, 2006. **8**(5): p. 669-680.
25. P. Karin, et al., Morphology and oxidation kinetics of CI engine's biodiesel particulate matters on cordierite Diesel Particulate Filters using TGA. *Int. J. Automot. Techn.*, 2017. **18**(1): p. 31-40.
26. K.H. Yoo, et al. "Experimental Studies of EGR Cooler Fouling on a GDI Engine", SAE Technical Paper, 2016-01-1090, 2016.
27. G. Fontana and E. Galloni, Experimental analysis of a spark-ignition engine using exhaust gas recycle at WOT operation. *Appl.Energ*, 2010. **87**(7): p. 2187-2193.
28. H. Wei, et al., Gasoline engine exhaust gas recirculation – A review. *Appl.Energ*, 2012. **99**: p. 534-544.
29. J.M. Luján, et al., Influence of a low pressure EGR loop on a gasoline turbocharged direct injection engine. *Appl.Therm.Eng*, 2015. **89**: p. 432-443.
30. W. Zeng, M. Sjöberg, and D.L. Reuss, Combined effects of flow/spray interactions and EGR on combustion variability for a stratified DISI engine. *Proc.Combust.Inst*, 2015. **35**(3): p. 2907-2914.
31. D. Fennell, J. Herreros, and A. Tsolakis, Improving gasoline direct injection (GDI) engine efficiency and emissions with hydrogen from exhaust gas fuel reforming. *Int. J. Hydrogen Energ*, 2014. **39**(10): p. 5153-5162.
32. T. Lattimore, et al., Investigation of EGR Effect on Combustion and PM Emissions in a DISI Engine. *Appl.Energ*, 2016. **161**: p. 256-267.
33. M. Hedge, et al., Effect of EGR on Particle Emissions from a GDI Engine. *SAE Int. J. Engines* 2011. **4**: p. 650-666.
34. C. Tornatore, et al., Optical diagnostics of the combustion process in a PFI SI boosted engine fueled with butanol–gasoline blend. *Energy*, 2012. **45**(1): p. 277-287.
35. R. Scarcelli, et al. "Cycle-to-Cycle Variations in Multi-Cycle Engine RANS Simulations", SAE Technical Paper, 2016-01-0593, 2016.
36. A. Irimescu, et al., Combustion process investigations in an optically accessible DISI engine fuelled with n-butanol during part load operation. *Renew.Energ*, 2015. **77**: p. 363-376.
37. K. Kondo, et al. "Uncertainty in Sampling and TEM Analysis of Soot Particles in Diesel Spray Flame", SAE Technical Paper, 2013-01-0908, 2013.
38. C.K. Gaddam and R.L. Vander Wal, Physical and chemical characterization of SIDI engine particulates. *Comb. Flame*, 2013. **160**(11): p. 2517-2528.
39. R. Daniel, et al., Ignition timing sensitivities of oxygenated biofuels compared to gasoline in a direct-injection SI engine. *Fuel*, 2012. **99**: p. 72-82.
40. E. Galloni, et al., Performance analyses of a spark-ignition engine firing with gasoline–butanol blends at partial load operation. *Energ.Convers.Manage*, 2016. **110**: p. 319-326.
41. M. Bogarra, et al., Study of particulate matter and gaseous emissions in gasoline direct injection engine using on-board exhaust gas fuel reforming. *Appl. Energ*, 2016. **180**: p. 245-255.
42. S.S. Merola, et al., Optical diagnostics of early flame development in a DISI (direct injection spark ignition) engine fueled with n-butanol and gasoline. *Energy*, 2016. **108**: p. 50-62.
43. X. Gu, et al., Emission characteristics of a spark-ignition engine fuelled with gasoline-n-butanol blends in combination with EGR. *Fuel*, 2012. **93**: p. 611-617.

44. J.M. Storey, et al., Novel Characterization of GDI Engine Exhaust for Gasoline and Mid-Level Gasoline-Alcohol Blends. *SAE Int. J. Fuels Lubr*, 2014. **7**: p. 571-579.
45. T. Alger, et al., The Role of EGR in PM Emissions from Gasoline Engines. *SAE Int. J. Fuels Lubr*, 2010. **3**: p. 85-98.
46. P. Karjalainen, et al., Exhaust particles of modern gasoline vehicles: A laboratory and an on-road study. *Atmos. Environ.*, 2014. **97**: p. 262-270.
47. T.L. Barone, et al., An analysis of direct-injection spark-ignition (DISI) soot morphology. *Atmos. Environ.*, 2012. **49**: p. 268-274.
48. M.A. Fayad, et al., Manipulating modern diesel engine particulate emission characteristics through butanol fuel blending and fuel injection strategies for efficient diesel oxidation catalysts. *Appl. Energ.*, 2017. **190**: p. 490-500.
49. H. Yang, et al., Experimental investigation into the oxidation reactivity and nanostructure of particulate matter from diesel engine fuelled with diesel/polyoxymethylene dimethyl ethers blends. *Sci. Rep.*, 2016. **6**: p. 37611.